Published in final edited form as:
Cereb Cortex. 2007 March ; 17(3): 702–712. doi:10.1093/cercor/bhk021.

Quantitative Analysis and Subcellular Distribution of mRNA and Protein Expression of the Hyperpolarization-Activated Cyclic Nucleotide-Gated Channels throughout Development in Rat Hippocampus

Amy L. Brewster[1], **Yuncai Chen**[1,2], **Roland A. Bender**[1,2], **Amy Yeh**[1], **Ryuichi Shigemoto**[3], and **Tallie Z. Baram**[1,2]

[1]Department of Anatomy and Neurobiology, University of California at Irvine, Irvine, CA 92697-4475, USA

[2]Department of Pediatrics, University of California at Irvine, Irvine, CA 92697-4475, USA

[3]Division of Cerebral Structure, National Institute for Physiological Sciences, Myodaiji, Okazaki 444-8787, Japan

Abstract

The properties of the hyperpolarization-activated current (I_h) and its roles in hippocampal network function evolve radically during development. Because I_h is conducted by the hyperpolarization-activated cyclic nucleotide-gated (HCN) cation channels, we tested the hypothesis that understanding the quantitative developmental profiles of HCN1, HCN2, and HCN4 expression, and the isoform- and age-specific progression of their subcellular distribution, should shed light on the established modifications of the properties of I_h throughout development. Combined quantitative in situ hybridization, regional western blots, and high-resolution, dual-label immunocy-tochemistry revealed striking and novel information about the expression and distribution of the HCN channel isoforms in the developing hippocampal formation. In cornus ammon 1 (CA) pyramidal cell layer, a robust increase of HCN1 mRNA and protein expression occurred with age, with reciprocal reduction of HCN4 and relatively stable HCN2 levels. These distinct expression patterns raised the contribution of HCN1 to the total HCN channel pool from 33% to 65% consonant with acceleration and reduced cyclic adenosine mono phosphate (cAMP) sensitivity of I_h in this region with age. In CA3, strong expression of HCN1 already neonatally supports the recently established role of this conductance in neonatal, age-specific, hippocampal oscillations (giant depolarizing potentials). Notably, HCN1 channels were present and probably transported to dendritic compartments already on postnatal day (P) 2, whereas HCN2 channel protein was not evident in dendrites for the first 2 weeks of life. HCN2 mRNA and protein expression remained fairly constant subsequent to the first week of life in all hippocampal subfields examined, whereas HCN4 mRNA and protein expression declined after maximal neonatal expression, so that the contribution of this isoform to the total HCN channel pool dropped from 43% (CA1) and 34% (CA3) on P11 to 8% (CA1) and 19% (CA3) on P90. Interneuronal expression of all HCN channel isoforms in stratum pyramidale was robust in parvalbumin-but not in cholecystokinin-expressing populations and with a subunit-specific subcellular distribution. Taken together, these data suggest that early in life, HCN4 may contribute

Address correspondence to Tallie Z. Baram, MD, PhD, Departments of Anatomy and Neurobiology and Pediatrics, University of California at Irvine, Irvine, CA 92697-4475, USA. tallie@uci.edu.
Amy L. Brewster and Yuncai Chen contributed equally to this work.

Conflict of interest: None declared.

significantly to the functions of I_h in specific hippocampal regions. In addition, these evolving, differential quantitative, and subcellular expression patterns of the HCN channel isoforms support age-specific properties and functions of I_h within the developing hippocampal formation.

Keywords

dendrites; hippocampus; development; hyperpolarization; ion channels; I_h

Introduction

In hippocampal neurons, cationic currents (I_h) conducted by hyperpolarization-activated cyclic nucleotide-gated (HCN, Clapham 1998) channels are involved in the regulation of intrinsic neuronal properties, including resting membrane potential (Maccaferri and others 1993; Lupica and others 2001), input resistance (Maccaferri and McBain 1996; Surges and others 2004), and dendritic summation (Magee 1998; Williams and Stuart 2000; Berger and others 2001; Poolos and others 2002). In mature hippocampus (as in other neuronal networks, e.g., Lüthi and McCormick 1998), I_h contributes to network function by promoting synchronized activity (Maccaferri and others 1993).

In neonatal hippocampus, both the properties of the h current and several of its functions differ from those in the adult and change with age (Strata and others 1997; Vasilyev and Barish 2002; Agmon and Wells 2003; Bender, Galindo, and others 2005). In addition, modifications of I_h properties in developing Cornus Ammon 1 (CA1) and CA3 pyramidal cells have been associated with pathological hyperexcitability and the generation of epilepsy (Chen and others 2001; Santoro and Baram 2003; Dubé and others 2006), suggesting that h current “functions” are at least partially determined by the biophysical properties of this conductance. These facts indicate that I_h plays important roles in both normal and pathological states in the developing hippocampal formation, requiring an understanding of the mechanisms that govern its properties.

A substantial body of evidence supports the notion that the characteristics of I_h in hippocampal neurons are governed by the relative contribution of the specific HCN channel isoforms to the composite of homomeric (and perhaps heteromeric, Much and others 2003; Brewster and others 2005) h channels (Franz and others 2000; Santoro and others 2000). Therefore, we tested the hypothesis that understanding the developmental expression patterns of the HCN channel iso-forms will provide important information about the properties of the current that is germane to its age-specific roles. Thus, presence of HCN expression in specific neuronal populations will permit putative assignment of functional roles to I_h, and absent expression will exclude proposed roles for this current (e.g., Strata and others 1997 vs. Bender, Galindo, and others 2005). In addition, the expression pattern of the channels will lead to an understanding of their regulation during pathological states. To study the complex developmental expression patterns of the HCN isoforms, we combined quantitative mRNA and protein analysis at regional and lamellar resolution with high-resolution immunocytochemistry (ICC), focusing also on age-dependent distribution (putative trafficking) patterns of these isoforms to subcellular compartments. We then validated the neuronal and subcellular location of each HCN channel isoform by using specific markers. The results revealed striking and novel information about the expression and age- and isoform-specific subcellular trafficking of the HCN channel isoforms in the developing hippocampal formation that explain the progressive changes in the properties of I_h in specific neuronal populations.

Materials and Methods

Animals

Sprague-Dawley–derived pregnant dams were maintained in a federally approved animal facility. Animals were housed in a quiet, uncrowded room under 12-h light/dark cycle (light on at 0700 h) with unlimited food and water. Delivery was verified at 12-h intervals (date of birth = day 0). On postnatal day (P) 2, litters were adjusted to 12 pups. When weaned (on P21), rats were housed 2–3 per cage. A total of 98 rats, at different ages, were used in these studies: P2 (n = 22), P11 (n = 28), P18 (n = 19), and P90 (n = 29). To control for potential effects of stress on HCN channel expression, rats were sacrificed within 10 min of their initial disturbance. All experimental procedures were approved by the University of California—Irvine Animal Care Committee in accordance with the National Institutes of Health guidelines.

Quantitative In Situ Hybridization

For in situ hybridization (ISH) procedures, rats were quickly decapitated on P2, P11, P18, or P90 (4–7 rats per group), and brains dissected and placed on powdered dry ice as described (Brewster and others 2002, 2005). Quantitative analyses of hippocampal HCN mRNA levels were accomplished using antisense ^{35}S-cRNA probes synthesized by in vitro transcription from cDNAs containing specific gene regions of mouse HCN1, HCN2, and HCN4 channels as previously described (Bender and others 2001; Brewster and others 2002). Briefly, coronal sections (20 μm) were cut, mounted on gel-coated slides, and fixed in 4% paraformaldehyde (PFA). Following a graded ethanol treatment, sections were exposed to acetic anhydride-triethanolamine and then dehydrated through 70–100% ethanol. Sections were preincubated in hybridization solution (50% formamide, 5× SET (sodium-EDTA-tris; 20× SET: 3 M NaCl, 0.05 M EDTA, 0.6 M Tris, pH 8) 0.2% sodium dodecyl sulfate, 5× Denhardt's solution, 0.5 mg/mL salmon sperm-sheared DNA, 250 mg/mL yeast tRNA, 100 mM dithiothreitol, 10% dextran sulfate) and probed overnight at 55 °C with antisense ^{35}S-cytidine triphosphate–radiolabeled HCN probes (0.5–1 × 10^6 cpm/30 μL/section). The specific activity of the probes was 1.67–5.2 × 10^9 cpm/μg. On the following day, sections were washed in decreasing concentrations of saline sodium citrate (SSC) solutions, with the most stringent wash at 0.03 × SSC for 60 min at 62 °C. Following dehydration in increasing alcohol concentrations, sections were apposed against Kodak Biomax films. Optimal exposure time was monitored using ^{14}C standards to maintain signal linearity. Specificity of signal was verified by hybridizing sections with sense probe or with excess unlabeled (100-fold) antisense probe in addition to labeled probe (Figs 1B, 4B and 7B)

Western Blot Procedures

For western blot analyses, each sample consisted of a hippocampal extract from an individual rat. Rats were rapidly decapitated at different developmental time points (P2, P11, P18, or P90; 4–7 rats per group), and hippocampi were quickly dissected. For regional analyses of protein expression in CA1 and dentate gyrus (DG) + CA3, hippocampi of P11 and P90 rats were further dissected as illustrated in Figure 2C (4–5 rats per group). Dissected tissue was immediately frozen in dry ice and then homogenized in glass/Teflon homogenizers in ice cold 0.32 M sucrose, 0.1 M Tris–HCl (pH 7.4) containing protease inhibitor cocktail (PIC, Complete™; diluted according to manufacturer's instructions; Roche, Alameda, CA). Samples were centrifuged at 1000 × g for 10 min at 4 °C, and pellet discarded. The resulting supernatant was centrifuged at 16 000 × g for 20 min at 4 °C, and the pellet containing membrane fractions resuspended in an artificial cerebrospinal fluid (124 mM NaCl, 3 mM KCl, 1.25 mM KH_2PO_4, 2.5 mM $MgSO_4$, 3.4 mM $CaCl_2$, 26 mM $NaHCO_3$, 10 mM glucose, 1 × PIC). Protein concentration was determined using Bio-Rad Protein assay (Bio-Rad, Hercules, CA). Equal amounts of protein were diluted in Laemmli

buffer, separated by sodium dodecyl sulfate–polyacrylamide gel electrophoresis (SDS-PAGE), and visualized using the enhanced chemiluminescence (ECL)-Plus kit (Amersham Pharmacia Biotech, Piscataway, NJ) as previously described (Brewster and others 2005). Briefly, 30 μg of protein extracts were separated on a 4–12% SDS-PAGE and transferred to Hybond-P polyvinyl difluoride membranes (Amersham Pharmacia Biotech). Membranes were blocked with 10% nonfat milk in 1× phosphate-buffered saline (PBS) overnight at 4 °C and were probed with rabbit anti-HCN1, rabbit anti-HCN2 (1:500 each; Chemicon, Temecula, CA), or rabbit anti-actin antisera (1:40 000; Sigma, St Louis, MO) overnight at 4 °C. For HCN4 detection, membranes were probed with guinea pig anti-HCN4 (1:500) for 1 h at room temperature as described in Notomi and Shigemoto (2004). Following washes in PBS-1% Tween (PBS-T) (3 × 5 min), membranes were incubated with secondary antibodies (donkey anti-rabbit IgG or rabbit anti-guinea pig IgG conjugated to horseradish peroxidase, 1:10 000; Amersham Pharmacia Biotech or Sigma, respectively) in PBS for 1 h at room temperature. Membranes were then washed in PBS-T (3 × 5 min) and incubated with ECL-Plus. Immunore-active bands were visualized by apposing membranes to Hyperfilm™ ECL (Amersham Pharmacia Biotech). Hippocampal extracts of individual rats of different age groups were run concurrently on the same gel. Specificity of signal was verified by preadsorbing primary antibodies with their respective antigens as well as by excluding the primary antibodies in the presence of the secondary antibodies. These treatments resulted in no immunoreactive-HCN bands (Figs 2C, 5C, and 8C; Notomi and Shigemoto 2004).

Immunocytochemistry

Rats (P2, P11, P18, and P90, $n = 3$ each group) were deeply anesthetized with sodium pentobarbital (100 mg/kg) and then transcardially perfused with 4% PFA (in 0.1 M phosphate buffer). Brains were removed, postfixed for 4 h in 4% PFA, cryoprotected with 25% sucrose, and frozen in dry ice. Coronal sections (20 μm) were then cut on a cryostat, and ICC was performed as described previously (Brewster and others 2002; Chen and others 2004). Briefly, free-floating sections were treated for 30 min with 0.3% H_2O_2 in PBS, washed (3 × 10 min) in PBS + 0.3% Triton-X (PBS-TX), and preincubated for 1 h with 3% normal goat serum/PBS-TX, followed by incubation with polyclonal rabbit anti-HCN1 (1:3000, Chemicon), polyclonal rabbit anti-HCN2 (1:2000, Notomi and Shigemo-to 2004), or polyclonal guinea pig anti-HCN4 (1:1000, Notomi and Shigemoto 2004) for 48 h at 4 °C. After 24 h, monoclonal mouse anti-parvalbumin (PV, 1:30 000, Chemicon), anti-glutamic acid decarboxylase (GAD65, 1:1000, Boehringer Mannheim), anti-cholecystokinin (CCK, 1:2000, CURE/Digestive Disease Research Center, UCLA), anti-microtubule–associated protein-2 (MAP-2, 1:8000, Chemicon), or anti-vesicular glutamate transporter 1 (VGLUT1, 1:5000, Chemicon) were added to the solution. Primary antibody binding was visualized with goat anti-rabbit IgG conjugated to Alexa Fluor 568 (HCN1, HCN2) in combination with goat anti-mouse IgG conjugated to Alexa Fluor 488 (MAP-2, PV, CCK; secondary antibody concentration: 1:200, each; Molecular Probes, Eugene, OR). For HCN4 detection, a biotinylated goat anti-guinea pig IgG secondary antibody (1:250, Vector, CA) was applied and detected with Alexa Fluor 568-conjugated streptavidin (Molecular Probes). Sections were then mounted onto gelatine-coated slides, embedded with Anti-Fading mounting medium (Biomeda, Foster City, CA), and coverslipped. Note that the antiserum used for HCN1 ICC was the same as the one used for western blots, so that the specificity controls provided in Figure 2 apply also to Figure 3. The antisera for HCN2 and HCN4 have been characterized previously (Notomi and Shigemoto 2004).

Images for Figures 3, 6, and 9 were acquired using a confocal microscope (Olympus, Fluoview, or Zeiss LSM510 META). For low-magnification views, surface scanning 15-μm thickness was employed (Figs 3A,B,E,F, 6A-D, and 9A-D). For high-magnification imaging, in Figures 3 and 6C,D(MAP-2-HCN1), G,H, all are 1-μm optical section imaging,

whereas GAD65–HCN1 and VGLUT–HCN1 images in *D* are 0.5 μm thick. In Figure 9, the high-magnification images in *E, F* were acquired from 1-μm thick virtual confocal sections.

Data Quantitation and Analyses

All quantitative analyses were performed by investigators unaware of the age group of the samples. Data acquisition and quantitation of ISH signals were carried out as described elsewhere (Brewster and others 2002; Bender and others 2003) on sections run concurrently. Quantitation and statistical analyses of HCN mRNA signal were accomplished by measuring optical density of incorporated radioactivity in pyramidal cell layer of CA1 and CA3 and in DG granule cell layer using the image analysis program Image Tool (UTHSC San Antonio, TX, version 1.27). Linearity of hybridization signal was ascertained using ^{14}C standards (American Radiolabeled Chemicals, St Louis, MO). Background signal was determined over the corpus callosum (HCN1, 17 ± 1.2 nCi/g; HCN2, 16 ± 1.4 nCi/g; HCN4, 14 ± 1.6 nCi/g) and subtracted from hybridization signal measured over the principal hippocampal cell layers. Western blot data acquisition and analysis were accomplished by measuring optical density of HCN1-, HCN2-, or HCN4-immunoreactive bands as described (Brewster and others 2005). Optical density of HCN bands derived from individual hippocampi was normalized to that of actin for each lane. In addition, actin levels in individual samples were quantified and used to normalize the relative amounts of HCN1, HCN2, and HCN4 in each sample. Statistical analyses for ISH and western blot data were performed with GraphPad Prism software (GraphPad Software, San Diego, CA) using *t*-test (if only 2 age groups were compared) or 1-factor analysis of variance followed by Bonferroni's post hoc test. Significance level was set at $P < 0.05$. All data are presented as means with standard errors.

Results

Quantitative Analysis of HCN1 mRNA Levels in Developing Hippocampus

Expression levels of the 3 HCN channel isoforms changed with development in an isoform-specific manner. HCN1 mRNA expression was detectable in the principal cell layers of all hippocampal regions already on P2 (Fig. 1A,B). At this age, intensity of HCN1 hybridization signal was more robust (~45% higher) in CA3 pyramidal cell layer compared with CA1 pyramidal cell layer or DG granule cell layer. During subsequent development, HCN1 mRNA abundance increased in hippocam-pal regions (CA1, CA3, and DG principal cell layers) with differing slopes and time courses. The most striking increase in HCN1 expression occurred in the CA1 pyramidal cell layer, where HCN1 mRNA levels were 2-fold higher on P11 and 3-fold higher on P90, compared with P2 (P2–P90: $F_{3,23} = 36.3$, $P < 0.001$; Fig. 1). In contrast, HCN1 gene expression in CA3 increased only modestly (~35%) during the same period (P2–P90; $F_{3,26} = 6.60$, $P < 0.01$). In granule cell layer, HCN1 expression did not change during the early postnatal period (P2–P11), but increased significantly (~2-fold) later (P11–P90; $F_{2,11} = 4.6$, $P < 0.05$). Thus, in mature hippocampus, HCN1 mRNA levels were higher than in the neonate in all regions, but the contribution of this isoform to the overall HCN channel mRNA pool was particularly high in area CA1 (an increase from ~30% to ~60%), consistent with the protein expression (see below) and the properties of the h current (Santoro and others 2000; Vasilyev and Barish 2002).

Quantitative Changes in HCN1 Protein Expression in Developing Hippocampus

Western blot analyses using equal protein amounts derived from whole hippocampi of individual rats revealed a progressive and significant increase in HCN1 protein levels with age (P2–P90: $F_{3,24} = 8.376$, $P < 0.001$; Fig. 2A). Hippocampal HCN1 protein levels were relatively low in the neonatal hippocampus, increased 2-fold between P2 and P11, and an additional 1.5-fold during the following week (P11–P18), reaching levels close to those of the adult (Fig. 2A, consonant with the mRNA in Fig. 1A). Because HCN1 protein is not

homogeneously expressed within the hippocampal formation (Santoro and others 2000; Brewster and others 2002; Lörincz and others 2002; and see above), protein expression was investigated separately in CA1 and DG + CA3 tissue blocks (as well as by high-resolution ICC, see below). As shown in Figure 2B, regional increases in protein expression levels were concordant with corresponding increases of mRNA signal. Thus, between P11 and P90, HCN1 protein levels increased ~70% in CA1 (mRNA increased 68%) and 111% in the DG + CA3 tissue, where mRNA increased ~48%. The proportionally higher developmental increase in HCN1 protein in the DG + CA3 tissue block compared with mRNA is likely a result of the fact that ISH analyses included only signal over principal cell layers, whereas protein analyses included also hilar neurons that begin to express HCN1 robustly during the second postnatal week (Bender and others 2001; Bender, Galindo, and others 2005).

Detailed and Subcellular Localization of HCN1 Channels in Developing Hippocampus

An important determinant of the function of the HCN channels involves their subcellular localization in neurons (Magee 1998; Williams and Stuart 2000; Berger and others 2001; Santoro and Baram 2003). Therefore, ICC was used to provide the requisite resolution (Figs 3,6, and 9). As expected, HCN1 immunore-activity was readily detectable in hippocampus already on P2 (Fig. 3A). Remarkably, already at this age, HCN1 channels localized to the dendrites of CA1 and CA3 pyramidal cells (Fig. 3A,C), resembling the mature pattern (Lörincz and others 2002; Notomi and Shigemoto 2004), and in distinct contrast to the pattern of HCN2 (see below). Dual labeling with MAP-2, a dendritic marker, supported this dendritic localization. Lack of colocalization of the channel with markers of glutamatergic presynaptic elements (VGLUT1) mitigated against the expression of the HCN1 channels in entorhinal afferent fibers to the dendrites of CA1 pyramidal cells (Fig. 3D). A modest colocalization of the HCN1 immunoreactivity with γ-aminobutyric acid-ergic (GABAergic) terminals (GAD65) was found on P11 but not on P2 (see punctate structures in Fig. 3D). This suggests that at this age, when expression of the HCN1 channel is already found in interneurons in CA1 and CA3 (Bender and others 2001; Bender, Galindo, and others 2005), HCN1 might exist in the axon terminals of a subset of these cell populations (and see below). These findings strongly support the dendritic localization of HCN1 channels and suggest that subcellular trafficking of the HCN1 channel isoform to the dendritic domain commences early in pyramidal cell differentiation (Tyzio and others 1999).

Indeed, in CA3 (and to a much lesser degree in CA1), in addition to expression within dendritic layers, HCN1 channels were robustly expressed in interneurons embedded within the pyramidal cell layer, where signal increased with age (Fig. 3G,H). Thus, most of the HCN1 signal observed over the pyramidal cell layer in the older ages (arrows in Fig. 3B,E) was attributable to expression of HCN1 channels in interneuronal axons densely innervating the somata of CA3 pyramidal cells (characteristic for basket cells, Fig. 3G,H). Interestingly, HCN1 channel expression in basket cell populations was highly selective: Dual-labeling ICC revealed that PV- but not CCK-expressing basket cells colocalized HCN1 (Fig. 3G,H).

Quantitative Analysis of HCN2 mRNA Levels in Developing Hippocampus

HCN2 mRNA expression was quite dissimilar to that of HCN1 (Fig. 4). Already on P2, modest HCN2 mRNA levels were expressed in CA1 and CA3 pyramidal cell layers, with low levels over the DG granule cell layer. In CA1, unlike the case for HCN1, HCN2 mRNA expression did not change significantly as a function of age (P2–P90: $F_{3,18} = 0.84$, $P > 0.05$). In CA3, where developmental increase for HCN1 was minimal, HCN2 mRNA expression increased by 114% between P2 and P11, achieving mature levels (P2–P90: $F_{3,14} = 8.4$, $P < 0.01$; P11 not significantly higher than later ages, P11–P90: $F_{2,12} = 3.7$, $P > 0.05$). In CA1, the relative contribution of this subunit to the total HCN mRNA pool declined by

~30% (from ~40% on P2 to ~30% on P90), whereas in CA3, the contribution of this isoform to the total HCN mRNA pool did not vary significantly with age.

Quantitative Expression of Hippocampal HCN2 Protein As a Function of Age

The developmental expression profile of hippocampal HCN2 protein was distinct from that of the HCN1 isoform. Levels increased 350% during the first 2 weeks of development (from 18.0 ± 4.2 on P2 to 80.0 ± 6.5 on P11 optical density units/actin; $P < 0.001$), whereas changes later in development were modest (P11–P90: $F_{2,17} = 2.6$, $P > 0.05$; Fig. 5A). At the regional level, HCN2 protein in CA1 reached mature expression levels already by P11 (concordant with the mRNA; compare Figs 4A and 5B). In DG + CA3, HCN2 protein expression did not consistently reflect the mRNA expression patterns, probably because mRNA was quantified over principal cell layers only, whereas protein analysis included also hilar interneurons and dendritic compartments.

Detailed and Subcellular Localization of HCN2 Channels in Developing Hippocampus

To resolve with higher precision, the developmental expression profile of the HCN2 channel protein, high-resolution ICC, and dual labeling were carried out. Consonant with the western blot analysis (Fig. 5A), little HCN2 protein was detectable on P2 using ICC (Fig. 6A). On P11, HCN2 signal was visible within somata of neurons embedded in the pyramidal cell layer of CA1 (Fig. 6B, inset). This expression occurred in both PV+ and PV– (presumed pyramidal) neurons. Signal within strata radia-tum and lacunosum-moleculare was modest at this age, and colocalization with the dendritic marker MAP-2 was not evident (Fig. 6E). Thus, compared with the early-onset dendritic localization and presumed trafficking of HCN1 (Fig. 3C), expression of HCN2 channels in the dendritic domain of CA1 pyramidal neurons commenced during a later developmental stage (Fig. 6E,F). Note that HCN2 immunoreactivity only partially overlapped the dendritic marker MAP-2; yet the channel did not seem to coreside with presynaptic markers of either GABAergic (GAD65) or glutamatergic (VGLUT1) neurons. A different progression of HCN2 expression pattern was found in CA3. Already on P11, HCN2 signal, strong over the pyramidal cell layer (arrows in Fig. 6B-D), was confirmed by confocal microscopy to emanate primarily from somata and axons of interneurons (Fig. 6G,H). For this channel, as for the HCN1 isoform, interneuronal expression was cell-type selective: PV-containing but never CCK-containing basket cells expressed HCN2 channels (Fig. 6G,H; note that not all HCN2-positive somata coexpressed PV). Pyramidal cell somata of CA3 were devoid of HCN2 (Notomi and Shigemoto 2004).

Quantitative Analysis of HCN4 mRNA Levels in Developing Hippocampus

HCN4 expression followed a distinctive developmental pattern. In general, HCN4 mRNA levels were lower (see expanded scale in Fig. 7A) and were maximal in neonatal hippocampus compared with later ages. Regional differences were noted: In CA1 pyramidal cell layer, expression declined precipitously with maturation (42% decline between P2 and P11 and 65% by P90; P2–P90: $F_{3,8} = 13.7$, $P < 0.001$; Fig. 7A,B). This time course contrasted sharply with the developmental profile of HCN4 expression in CA3, where low signal on P2 doubled by P11 (P2–P11; $P < 0.001$; P11–P90: $F_{2,7} = 0.42$, $P > 0.05$; Fig. 7A,B), and in granule cell layer, where HCN4 mRNA levels remained relatively constant throughout postnatal development (P2–P90: $F_{3,8} = 1.7$, $P > 0.05$; Fig. 7A,B). Thus, the overall contribution of HCN4 to the HCN channel pool plunged in CA1 pyramidal layer neurons from 30% to 8%, consistent with substantial acceleration of the h current kinetics with age.

Quantitative Expression of HCN4 Protein in Developing Hippocampus

Protein levels of HCN4 in the whole hippocampal formation were generally concordant with the mRNA pattern, being highest in early postnatal hippocampus (P2–P90: $F_{3,12} = 36.5$, $P < 0.0001$; Fig. 8A). Thus, on P2, HCN4 protein levels were 5-fold higher than those in mature hippocampus ($P < 0.001$). The major drop occurred between P11 and P18 (50%, $P < 0.05$, Fig. 8A), an age of major changes in the mechanisms of hyper-polarization (and h channel activation) in the hippocampal formation (Ben-Ari 2002). At the regional level, most HCN4 protein was expressed in CA1, where levels declined sharply between P11 and P90 (80%, *t*-test: $P < 0.001$, Fig. 8B), whereas the low levels of protein and mRNA in DG + CA3 did not change significantly with age (*t*-test: $P > 0.05$, Figs 7A and 8B).

Detailed and Subcellular Localization of HCN4 Channels in Developing Hippocampus

ICC studies of HCN4 expression confirmed a much lower expression of this isoform compared with the others (Fig. 9A–D). Interestingly, low-HCN4 immunoreactivity occurred in CA1 of P2 (Fig. 9A) and P11 (Fig. 9B) hippocampus when western blots suggested a higher expression, and the reasons are not entirely clear. In contradistinction to both HCN1 and HCN2, dual labeling with MAP-2 did not provide evidence for a dendritic localization of HCN4 channels on P2 (Fig. 9E) or later in development (not shown). HCN4-expressing interneurons were identified as early as P11 and were clearly visible by P18 (Fig. 9C). Within CA3, these interneurons were mainly associated with the pyramidal cell layer and, similar to HCN1 and HCN2, coexpressed PV (Fig. 9F) but not CCK. In contrast to the situation with HCN1 and HCN2, HCN4 protein expression was confined primarily to the somata of these basket cells and was rarely detected in axon terminals (Fig. 9F).

Discussion

The major findings of this study are as follows: 1) Quantitative expression patterns of HCN1, HCN2, and HCN4 channel iso-forms undergo distinct progressions in developing hippocampus. 2) For each isoform, expression evolves differentially within hippocampal regions and subcellular domains, as evident from quantitative mRNA and protein analyses, as well as from fine-structural and dual-labeled immunocytochemical studies. 3) Thus, the relative contribution of each isoform to the channel makeup of I_h is tightly and selectively regulated by age within each hippocampal region, neuronal population, and subcellular domain. These complex patterns of HCN channel isoform expression should influence the properties of I_h within neuronal populations and cellular domains of the maturing hippocampal formation, which, in turn, contribute to its age-dependent functions (Bender, Galindo, and others 2005).

Spatiotemporal expression patterns of the HCN channels in the mature and developing hippocampus have only been described qualitatively (e.g., Ludwig and others 1998; Moosmang and others 1999; Santoro and others 2000; Bender and others 2001; Vasilyev and Barish 2002; Notomi and Shigemoto 2004). Other studies have shown developmental regulation of the expression of HCN channels (Bender and others 2001) and of I_h (Vasilyev and Barish 2002). Because the properties of I_h that evolve with maturation are largely governed by the isoform “makeup” of the h channels (reviewed in Santoro and Baram 2003), this study relied on several combined approaches to provide a full understanding of HCN isoform expression in the developing hippocampus.

Quantitative estimates of HCN1, HCN2, and HCN4 mRNA and protein expression in the hippocampal CA1 region demonstrates a “molecular switch” from a preponderance of slow kinetics, cAMP-sensitive isoforms (HCN2 and HCN4) to a major contribution of fast kinetics, cAMP-insensitive isoforms. Indeed, in CA1 pyramidal cells, I_h activation and

deactivation kinetics accelerate with age (Vasilyev and Barish 2002), likely reflecting the progressively increasing contribution of the HCN1 isoform to the total cellular current (Santoro and others 2000; Chen and others 2001) in the face of stable HCN2 expression and declining HCN4 levels. High-resolution ICC further hones these observations, showing that they apply primarily to the somatic compartments.

The use of high-resolution confocal microscopy as well as dual labeling to study the age specificity and cell-type selectivity of HCN isoform expression in distinct subcellular compartments yielded novel and interesting findings about the differential trafficking of each HCN isoform to the dendritic compartment as a function of age: Thus, though HCN1, HCN2, and HCN4 were expressed in CA1 pyramidal cells already during the first postnatal week, only HCN1 resided in dendritic layers of CA1, colocalized with the dendritic marker MAP-2 and not with afferent glutamatergic and GABAergic axon terminals during the first postnatal week, whereas showing modest colocaliza-tion with GAD65 during the second week of life (Fig. 3C,D). In contrast, HCN2 immunoreactivity occurred in dendritic domains later in development (Fig. 6), and HCN4 was not detected in dendritic domains at any age (Fig. 9). This early postnatal distribution of the channels is highly distinct from the adult pattern, where both HCN1 and HCN2 channels localize to the distal dendrites of CA1 pyramidal cells (Santoro and others 1997; Brewster and others 2002; Lörincz and others 2002; Notomi and Shigemoto 2004; Figs 3F and 6D).

Whereas the possibility that the HCN channels are locally synthesized within dendrites cannot be excluded (for review, see Steward and Worley 2002), our previous studies, looking at subcellular distribution of HCN mRNA expression using colorimetric ISH, failed to detect HCN1 mRNA in dendrites or dendritic layers (Bender and others 2001) and showed strong mRNA expression within the cell body. Although the sensitivity of this method may not suffice to detect low levels of dendritic mRNA, the large majority of HCN1-type channels are found in dendrites, suggesting that if the majority of translation were to occur in dendrites, HCN1 mRNA should not be found solely in the soma. Therefore, the differential age-specific localization of HCN1 and HCN2 isoforms in dendrites is likely to be a result of differential subcellular trafficking. The mechanism for delayed dendritic trafficking of HCN2 channels and the absence of HCN4 transport are unclear as yet. Subcellular trafficking of ion channels is generally regulated by posttranslational mechanisms (Heusser and Schwappach 2005). In the case of HCN channels, interacting proteins, including MiRP1 and TRIP8b, have been suggested to regulate subcellular trafficking (Qu and others 2004; Santoro and others 2004). In future studies, it will be interesting to investigate whether dendritic trafficking of HCN channels requires expression of specific interacting proteins that themselves may undergo developmental maturation.

These findings imply that dendritic HCN channels during the first week of life are composed virtually only of HCN1 channel isoforms, whereas by the end of the third postnatal week dendritic h current is carried by both HCN1- and HCN2-type channel isoforms. Importantly, these findings suggest that dendritic I_h in pyramidal cells from developing hippocampus might have properties that are highly distinct from those of somatic currents as well as from those of dendritic currents in, for example, CA1 pyramidal cells of mature hippocampus (Magee and others 1998; Poolos and others 2002; Bender, Galindo, and others 2005).

In CA3 pyramidal cell layer, the quantitative expression of HCN2 mRNA and protein remained relatively high, with persistent significant contribution to the total HCN channel pool. Indeed, I_h kinetics have been found to be slower than those in CA1 during the first 3 postnatal weeks (Vasilyev and Barish 2002). Here, high-resolution and dual-label ICC demonstrate, for the first time, the localization of the HCN1, HCN2, and HCN4 channel isoforms in defined interneuronal populations within hippocampal CA3. We found

expression of all 3 isoforms in apparent basket cells, consistent with Notomi and Shigemoto (2004). In addition, we found that expression patterns were isoform specific and cell-type selective: Thus, HCN1 and HCN2 channels frequently localized to PV-containing axon terminals but were never seen in terminals expressing CCK (Figs 3G,H and 6G,H). HCN4 immunoreactivity, although present in the same basket cell population, was generally confined to the somatic region of these interneurons. PV- and CCK-expressing basket cells constitute 2 nonoverlapping populations of interneurons with similar morphology but distinct physiological properties and network functions (Freund 2003). PV-containing basket cells are fast spiking, capable of firing with frequencies >100 Hz, whereas the CCK-containing population is unable to fire such high frequencies without accommodation. HCN channels within axon terminals enhance the probability and regularity of neurotransmitter release (Beaumont and Zucker 2000; Southan and others 2000; Agmon and Wells 2003) and may thus contribute to the functions of the PV-containing population.

In general, HCN1 and HCN4 protein expression correlated well with the corresponding mRNA patterns (Figs 1A and 2B for HCN1, Figs 7A and 8B for HCN4; see also Brewster and others 2005, for HCN1), suggesting that transcriptional regulation is an important determinant of the amount of HCN1 and HCN4 channels in hippocampal neurons. In contrast, HCN2 protein expression did not consistently reflect the mRNA expression pattern: HCN2 protein levels in CA3 were lower than expected from the mRNA expression, as determined by ISH analysis (Figs 4A and 5B). Similar inconsistencies regarding HCN2 mRNA/protein relationships have been observed after seizure-induced enhancement of hippocampal HCN2 mRNA expression, which did not result in altered HCN2 protein levels (Brewster and others 2005). In addition, Santoro and others (2000) failed to detect I_h currents in CA3 pyramidal neurons despite a strong HCN2 mRNA expression over the CA3 pyramidal cell layer (but see Fisahn and others 2002; Cobb and others 2003). Whereas the reasons for this HCN2 mRNA and protein mismatch are not clear, they may be a result of incomplete mRNA translation, enhanced protein degradation, and/or other posttranslational regulatory mechanisms (Much and others 2003; Brewster and others 2005).

In summary, this study is the first to quantify at the mRNA and protein levels, the developmental expression patterns of HCN1, HCN2, and HCN4, and to investigate the modulation of the subcellular distribution of these intrinsic neuronal channels. The progressive, differential, quantitative, and subcellular expression patterns of the HCN channel isoforms found here indicate strong transcriptional and posttranslational regulation of the expression of these channels. In addition, they support age-specific properties and functions of I_h within the maturing hippocampal formation (Ben-Ari 2001; Agmon and Wells 2003; Bender, Galindo, and others 2005).

Acknowledgments

The authors are grateful to Dr Celine Dubé and to Nisha Patel for help with dissections and to Michele Hinojosa for excellent editorial support. This work was supported by the National Institutes of Health NS 47993 (ALB) and NS 35439 (TZB).

References

Agmon A, Wells JE. The role of the hyperpolarization-activated cationic current I(h) in the timing of interictal bursts in the neonatal hippocampus. J Neurosci. 2003; 23:3658–3668. [PubMed: 12736337]

Beaumont V, Zucker RS. Enhancement of synaptic transmission by cyclic AMP modulation of presynaptic Ih channels. Nat Neurosci. 2000; 3:133–141. [PubMed: 10649568]

Ben-Ari Y. Developing networks play a similar melody. Trends Neurosci. 2001; 24:353–360. [PubMed: 11356508]

Ben-Ari Y. Excitatory actions of gaba during development: the nature of the nurture. Nat Rev Neurosci. 2002; 3:728–739. [PubMed: 12209121]

Bender RA, Brewster AL, Santoro B, Ludwig A, Hofmann F, Biel M, Baram TZ. Differential and age-dependent expression of hyperpolarization-activated, cyclic nucleotide-gated cation channel isoforms 1-4 suggests evolving roles in the developing rat hippocampus. Neuroscience. 2001; 106:689–698. [PubMed: 11682156]

Bender RA, Galindo R, Mameli M, Gonzalez-Vega R, Valenzuela CF, Baram TZ. Synchronized network activity in developing rat hippocampus involves regional hyperpolarization-activated cyclic nucleotide gated (HCN) channel function. Eur J Neurosci. 2005; 22:2667–2674.

Bender, RA.; Kretz, O.; Patel, N.; Richichi, R.; Frotscher, M.; Baram, TZ. Online Program No 377.13, 2005 Abstract Viewer/Itinerary Planner. Washington, DC: Society for Neuroscience; 2005. Activity-dependent regulation of hyperpolarization-activated cyclic nucleotide-gated (HCN) 1 channel transport in axons of rat perforant path.

Bender RA, Soleymani SV, Brewster AL, Nguyen ST, Beck H, Mathern GW, Baram TZ. Enhanced expression of a specific hyperpolarization-activated cyclic nucleotide-gated cation channel (HCN) in surviving dentate gyrus granule cells of human and experimental epileptic hippocampus. J Neurosci. 2003; 23:6826–6836. [PubMed: 12890777]

Berger T, Larkum ME, Lüscher HR. High I(h) channel density in the distal apical dendrite of layer V pyramidal cells increases bidirectional attenuation of EPSPs. J Neurophysiol. 2001; 85:855–868. [PubMed: 11160518]

Brewster AL, Bender RA, Chen Y, Dubé C, Eghbal-Ahmadi M, Baram TZ. Developmental febrile seizures modulate hippocampal gene expression of hyperpolarization-activated channels in an isoform and cell-specific manner. J Neurosci. 2002; 22:4591–4599. [PubMed: 12040066]

Brewster AL, Bernard JA, Gall CM, Baram TZ. Formation of heteromeric hyperpolarization-activated cyclic nucleotide-gated (HCN) channels in the hippocampus is regulated by developmental seizures. Neurobiol Dis. 2005; 19:200–207. [PubMed: 15837575]

Chen K, Aradi I, Thon N, Eghbal-Ahmadi M, Baram TZ, Soltesz I. Persistently modified h-channels after complex febrile seizures convert the seizure-induced enhancement of inhibition to hyperexcitability. Nat Med. 2001; 7:331–337. [PubMed: 11231632]

Chen S, Wang J, Siegelbaum SA. Properties of hyperpolarization-activated pacemaker current defined by coassembly of HCN1 and HCN2 subunits and basal modulation by cyclic nucleotide. J Gen Physiol. 2001; 117:491–503. [PubMed: 11331358]

Chen Y, Bender RA, Brunson KL, Pomper J, Grigoriadis DE, Wurst W, Baram TZ. Modulation of dendritic differentiation by corticotropin-releasing factor in the developing hippocampus. Proc Natl Acad Sci USA. 2004; 101:15782–15787. [PubMed: 15496472]

Clapham DE. Not so funny anymore: pacing channels are cloned. Neuron. 1998; 21:5–7. [PubMed: 9697846]

Cobb SR, Larkman PM, Bulters DO, Oliver L, Gill CH, Davies CH. Activation of Ih is necessary for patterning of mGluR and mAChR induced network activity in the hippocampal CA3 region. Neuro-pharmacology. 2003; 44:293–303.

Dubé C, Richichi C, Bender RA, Chung G, Litt B, Baram TZ. Temporal lobe epilepsy after experimental prolonged febrile seizures: prospective analysis. Brain. 2006; 129:911–922. [PubMed: 16446281]

Fisahn A, Yamada M, Duttaroy A, Gan JW, Deng CX, McBain CJ, Wess J. Muscarinic induction of hippocampal gamma oscillations requires coupling of the M1 receptor to two mixed cation currents. Neuron. 2002; 33:615–624. [PubMed: 11856534]

Franz O, Liss B, Neu A, Roeper J. Single-cell mRNA expression of HCN1 correlates with a fast gating phenotype of hyperpolarization-activated cyclic nucleotide-gated ion channels (Ih) in central neurons. Eur J Neurosci. 2000; 12:2685–2693. [PubMed: 10971612]

Freund TF. Interneuron diversity series: rhythm and mood in perisomatic inhibition. Trends Neurosci. 2003; 26:489–495. [PubMed: 12948660]

Heusser K, Schwappach B. Trafficking of potassium channels. Curr Opin Neurobiol. 2005; 15:364–369. [PubMed: 15961040]

Lörincz A, Notomi T, Tamas G, Shigemoto R, Nusser Z. Polarized and compartment-dependent distribution of HCN1 in pyramidal cell dendrites. Nat Neurosci. 2002; 5:1185–1193. [PubMed: 12389030]

Ludwig A, Zong X, Jeglitsch M, Hofmann F, Biel M. A family of hyperpolarization-activated mammalian cation channels. Nature. 1998; 393:587–591. [PubMed: 9634236]

Lupica CR, Bell JA, Hoffman AF, Watson PL. Contribution of the hyperpolarization-activated current (I_h) to membrane potential and GABA release in hippocampal interneurons. J Neurophysiol. 2001; 86:261–268. [PubMed: 11431507]

Lüthi A, McCormick DA. H-current: properties of a neuronal and network pacemaker. Neuron. 1998; 21:9–12. [PubMed: 9697847]

Maccaferri G, Mangoni M, Lazzari A, DiFrancesco D. Properties of the hyperpolarization-activated current in rat hippocampal CA1 pyramidal cells. J Neurophysiol. 1993; 69:2129–2136. [PubMed: 7688802]

Maccaferri G, McBain CJ. The hyperpolarization-activated current (I_h) and its contribution to pacemaker activity in rat CA1 hippocampal stratum oriens-alveus interneurons. J Physiol. 1996; 497:119–130. [PubMed: 8951716]

Magee JC. Dendritic hyperpolarization-activated currents modify the integrative properties of hippocampal CA1 pyramidal neurons. J Neurosci. 1998; 18:7613–7624. [PubMed: 9742133]

Moosmang S, Biel M, Hofmann F, Ludwig A. Differential distribution of four hyperpolarization-activated cation channels in mouse brains. Biol Chem. 1999; 380:975–980. [PubMed: 10494850]

Much B, Wahl-Schott C, Zong X, Schneider A, Baumann L, Moosmang S, Ludwig A, Biel M. Role of subunit heteromerization and N-linked glycosylation in the formation of functional hyperpolarization-activated cyclic nucleotide-gated channels. J Biol Chem. 2003; 278:43781–43786. [PubMed: 12928435]

Notomi T, Shigemoto R. Immunohistochemical localization of Ih channel subunits, HCN1-4, in the rat brain. J Comp Neurol. 2004; 471:241–276. [PubMed: 14991560]

Poolos NP, Migliore M, Johnston D. Pharmacological up-regulation of h-channels reduces the excitability of pyramidal neuron dendrites. Nat Neurosci. 2002; 5:767–774. [PubMed: 12118259]

Qu J, Kryukova Y, Potapova IA, Doronn SV, Larsen M, Krishnamurthy G, Cohen IS, Robinson RB. MiRP1 modulates HCN2 channel expression and gating in cardiac myocytes. J Biol Chem. 2004; 279:43497–43502. [PubMed: 15292247]

Santoro B, Baram TZ. The multiple personalities of h-channels. Trends Neurosci. 2003; 26:550–554. [PubMed: 14522148]

Santoro B, Chen S, Luthi A, Pavlidis P, Shumyatsky GP, Tibbs GR, Siegelbaum SA. Molecular and functional heterogeneity of hyperpolarization-activated pacemaker channels in the mouse CNS. J Neurosci. 2000; 20:5264–5275. [PubMed: 10884310]

Santoro B, Grant SGN, Bartsch D, Kandel ER. Interactive cloning with the SH3 domain of N-src identifies a new brain specific ion channel protein, with homology to eag and cyclic nucleotide-gated channels. Proc Natl Acad Sci USA. 1997; 94:14815–14820. [PubMed: 9405696]

Santoro B, Wainger BJ, Siegelbaum SA. Regulation of HCN channel surface expression by a novel C-terminal protein-protein interaction. J Neurosci. 2004; 24:10750–10762. [PubMed: 15564593]

Southan AP, Morris NP, Stevens GJ, Robertson B. Hyperpolarization-activated currents in presynaptic terminals of mouse cerebellar basket cells. J Physiol. 2000; 526:91–97. [PubMed: 10878102]

Steward O, Worley P. Local synthesis of proteins at synaptic sites on dendrites: role in synaptic plasticity and memory consolidation? Neurobiol Learn Mem. 2002; 78:508–527. [PubMed: 12559831]

Strata F, Atzori M, Molnar M, Ugolini G, Tempia F, Cherubini E. A pacemaker current in dye-coupled hilar interneurons contributes to the generation of giant GABAergic potentials in developing hippocampus. J Neurosci. 1997; 17:1435–1446. [PubMed: 9006985]

Surges R, Freiman TM, Feuerstein TJ. Input resistance is voltage dependent due to activation of Ih channels in rat CA1 pyramidal cells. J Neurosci Res. 2004; 76:475–480. [PubMed: 15114619]

Tyzio R, Represa A, Jorquera I, Ben-Ari Y, Gozlan H, Aniksztejn L. The establishment of GABAergic and glutamatergic synapses on CA1 pyramidal neurons is sequential and correlates with the development of the apical dendrite. J Neurosci. 1999; 19:10372–10382. [PubMed: 10575034]

Vasilyev DV, Barish ME. Postnatal development of the hyperpolarization-activated excitatory current Ih in mouse hippocampal pyramidal neurons. J Neurosci. 2002; 22:8992–9004. [PubMed: 12388606]

Williams SR, Stuart JG. Site independence of EPSP time course is mediated by dendritic Ih in neocortical pyramidal neurons. J Neurophysiol. 2000; 83:3177–3182. [PubMed: 10805715]

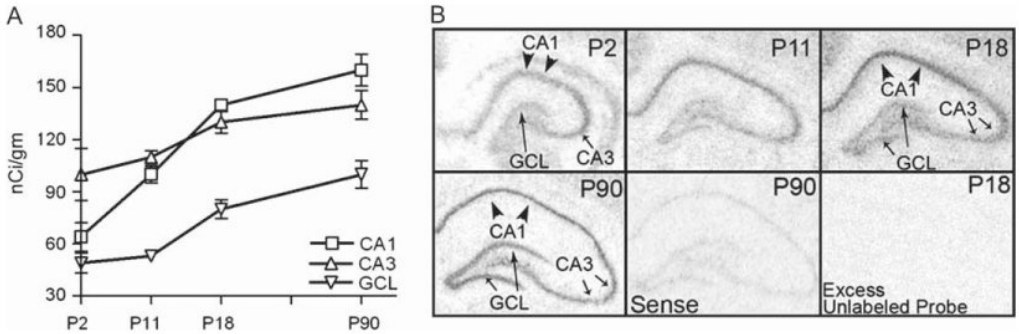

Figure 1.

Quantitative ISH analyses of HCN1 mRNA expression in developing hippocampus. (*A*) Expression increases progressively with age in pyramidal cell layers of CA1 and CA3 and in DG granule cell layer (GCL). This increase is particularly pronounced in CA1 (P2–P90: ~250%). (*B*) Representative autoradiographs showing hippocampal HCN1 mRNA signal on P2, P11, P18, and P90 and the results of control ISH experiments using sense probe or excess (100×) unlabeled antisense probe in addition to labeled probe.

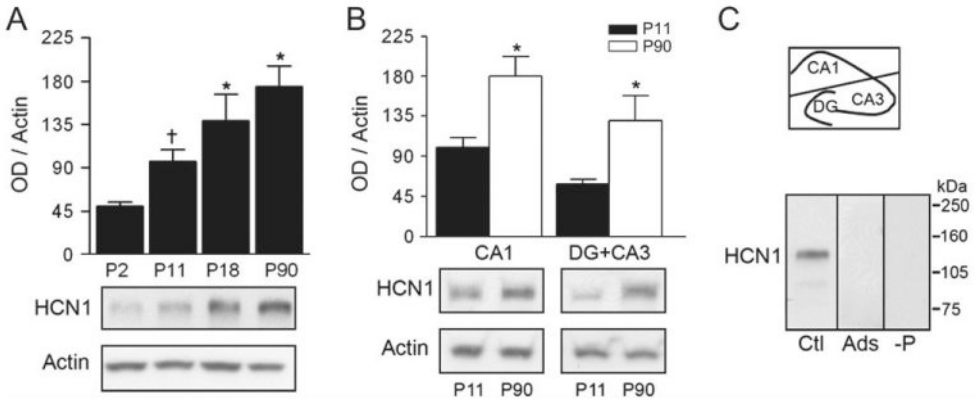

Figure 2.

Quantitative western blot analyses of HCN1 protein expression in developing hippocampus. (*A*) Top: In whole hippocampus, HCN1 protein levels increase steadily between P2 and P90. Bottom: Representative western blot. Optical density (OD) of HCN1-immunoreactive bands was normalized to that of actin for each lane (*denotes significance when compared with P2, †denotes significance when compared with P90; *t*-test: $P < 0.05$). (*B*) Top: Analysis of regional HCN1 protein expression in isolated CA1 or DG + CA3 demonstrates that protein levels increase proportionally with mRNA levels in these regions (CA1: ~70%, DG + CA3: ~111%, compare with Fig. 1B). Bottom: Representative western blots illustrate significantly higher HCN1 protein levels in both CA1 and DG + CA3 in a P90 compared with a P11 rat (*denotes significance between age groups; *t*-test: $P < 0.05$). (*C*) Top: Schematic illustration of dissection procedure for regional analyses. Bottom: Immunoreactive HCN1 bands (Ctl) have an apparent molecular weight of ~120 kDa. Preadsorption (Ads) with antigen or excluding HCN1 antisera (-P) in the presence of the secondary antibody abolishes immunoreactivity.

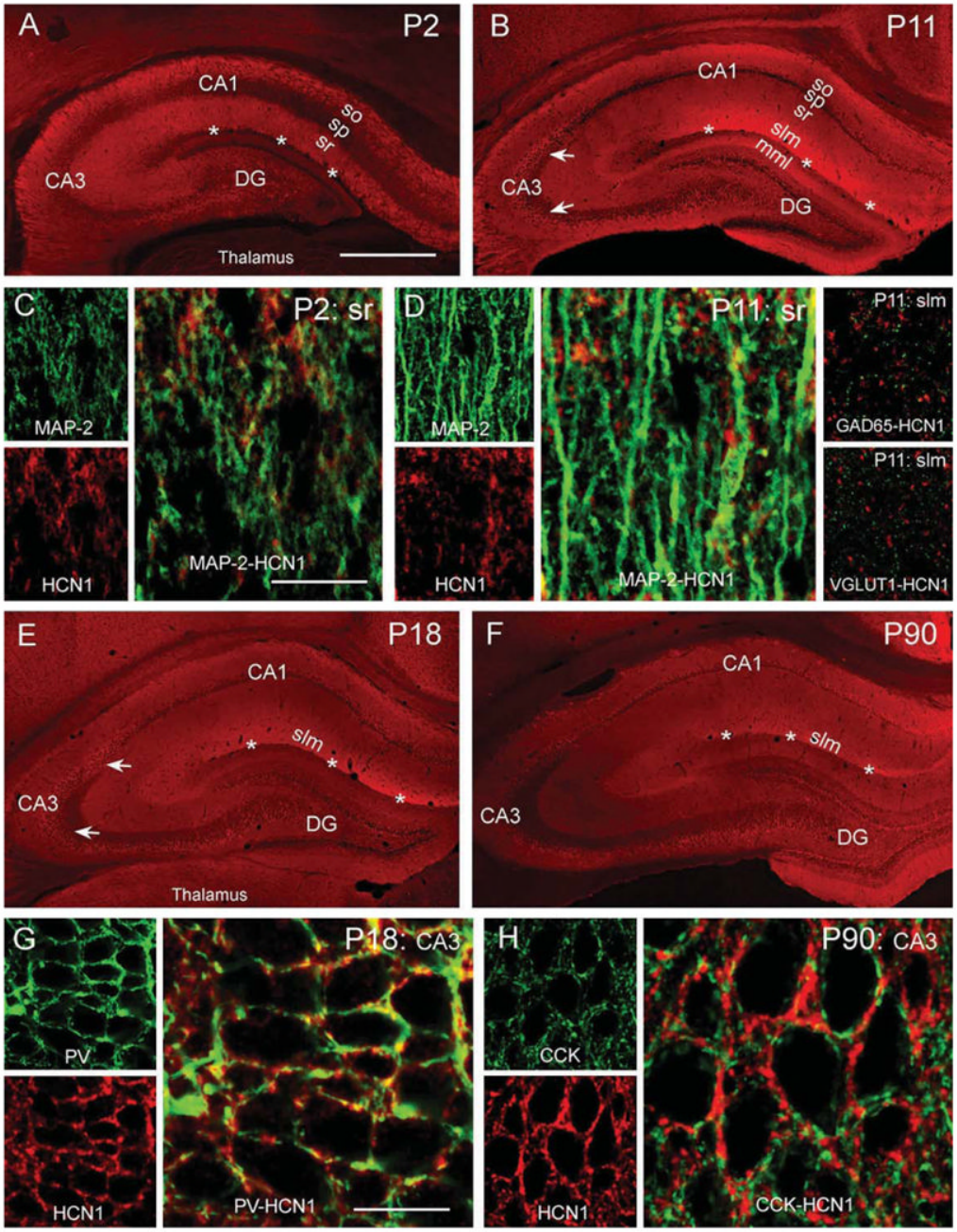

Figure 3.

Subcellular localization of HCN1 channels in developing hippocampus. (*A*, *B*) Low-magnification photographs demonstrate that HCN1 channels are localized in the dendritic field of CA1 pyramidal cells as early as P2 (*A*) found in both stratum radiatum as well as in stratum lacunosum-moleculare (slm,*B*). On P11, but not later, HCN1 signal is also observed in the medial molecular layer (mml) of DG, where the signal is likely within the axons of the perforant path (Bender, Kretz, and others 2005). (*C*, *D*) Dual labeling of HCN1 (red) and the dendritic marker MAP-2 (green) on P2 (*C*) and P11 (*D*) reveals that most HCN1 coresides with the dendritic marker. In contrast, dual labeling of HCN1 with presynaptic markers of afferents to the CA1 dendrites failed to demonstrate a presynaptic location of HCN1 in

VGLUT1-containing terminals, whereas a modest colocalization of the HCN1 immunoreactivity with GABAergic terminals (GAD65) was found on P11 but not on P2 (*D*). (*E*) By P18, the HCN1 distribution pattern strongly resembles the mature pattern (*F*) characterized by a robust expression of HCN1 channels in the distal dendritic field of CA1 (slm) and by pronounced HCN1 signal in CA3 (arrows in *B*,*E*,*F*). (*G*, *H*) HCN1 signal in the pyramidal cell layer (particularly in CA3) is mainly attributable to expression of the channels in axons of basket cells. Dual labeling of HCN1 (red) and PV (green in *G*) or CCK (green in *H*) reveals that HCN1 frequently localizes to axonal terminals of PV-expressing basket cells (*G*) but never to terminals that contain CCK (*H*). sp, stratum pyramidale; so, stratum oriens; asterisks demarcate the hippocampal fissure. Confocal microscopy virtual slice thicknesses:(*A*,*B*,*E*,*F*) = 15 μm (surface scanning), (*C*, *D*) (MAP-2-HCN1) and (*G*, *H*) = 1 μm. (*D*) GAD65 and VGLUT dual labeling with HCN1 = 0.5 μm. Scale bar:(*A*,*B*,*E*,*F*) = 900 μm; (*C*) = 27 μm (left panels), 13.5 μm (right panel); (*D*) = 27 μm (left and right panels), 13.5 μm (middle panel); (*G*, *H*) = 40 μm (left panels), 20 μm (right panel).

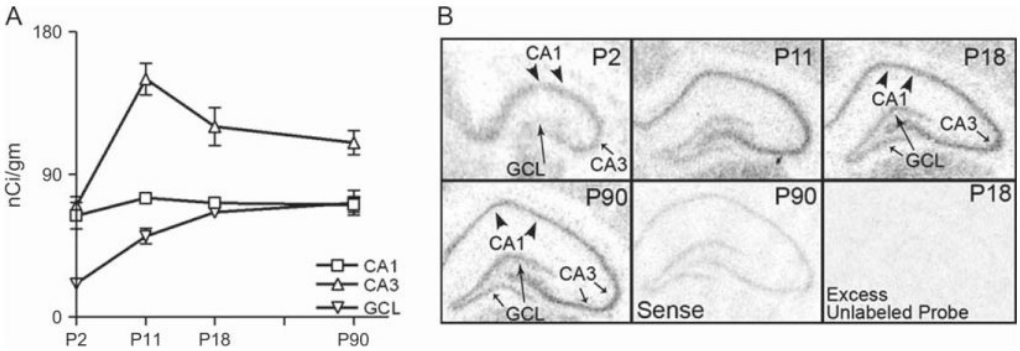

Figure 4.

Quantitative ISH analyses of HCN2 mRNA expression in developing hippocampus. (*A*) Expression levels of HCN2 mRNA evolve differentially in hippocampal regions: Expression remains relatively constant in CA1 pyramidal cell layer, whereas it increases with age in CA3 and DG principal cell layers. In CA3, HCN2 mRNA expression increases during the second postnatal week reaching mature levels by P11. (*B*) Representative autoradiographs show hippocampal HCN2 mRNA signal on P2, P11, P18, and P90 and the results of control ISH experiments using sense probe or excess (100×) unlabeled antisense probe in addition to labeled probe.

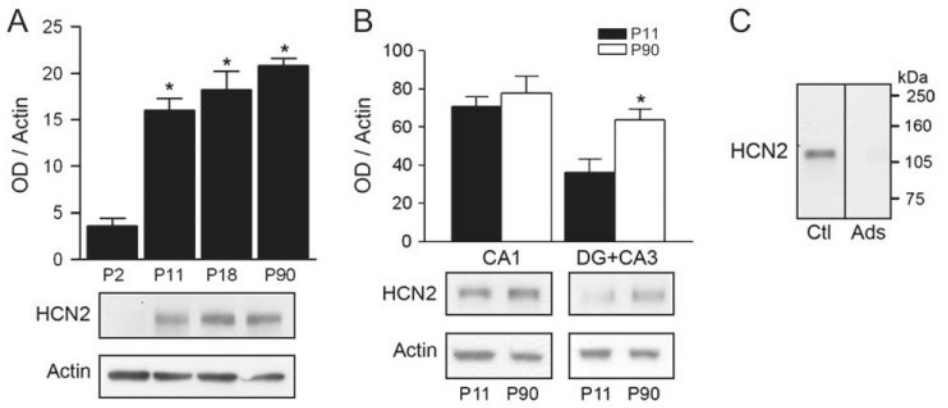

Figure 5.

Quantitative western blot analyses of HCN2 protein expression in developing hippocampus. (*A*) Top: In whole hippocampus, HCN2 protein levels are relatively low on P2, increase between P2 and P11, but not thereafter. Bottom: Representative western blot. Optical density (OD) of HCN2-immunoreactive bands was normalized to that of actin for each lane (*denotes significance when compared with P2, $P < 0.05$). (*B*) Top: Regional analyses reveal that HCN2 protein and mRNA expression (see Fig. 4A) are comparable in CA1. However, in DG + CA3, HCN2 protein levels are significantly higher on P90 compared with P11, in contrast to mRNA levels (*denotes significance between groups; *t*-test: $P < 0.05$). Bottom: Representative western blots. (*C*) Immunoreactive-HCN2 bands (Ctl) have an apparent molecular weight of ~115 kDa. Preadsorption (Ads) with antigen abolishes immunoreactivity. Note that because both HCN1 and HCN2 are detected using the same secondary antibody (anti-rabbit IgG), a control experiment omitting the primary antibody is provided for HCN1 only (Fig. 2C).

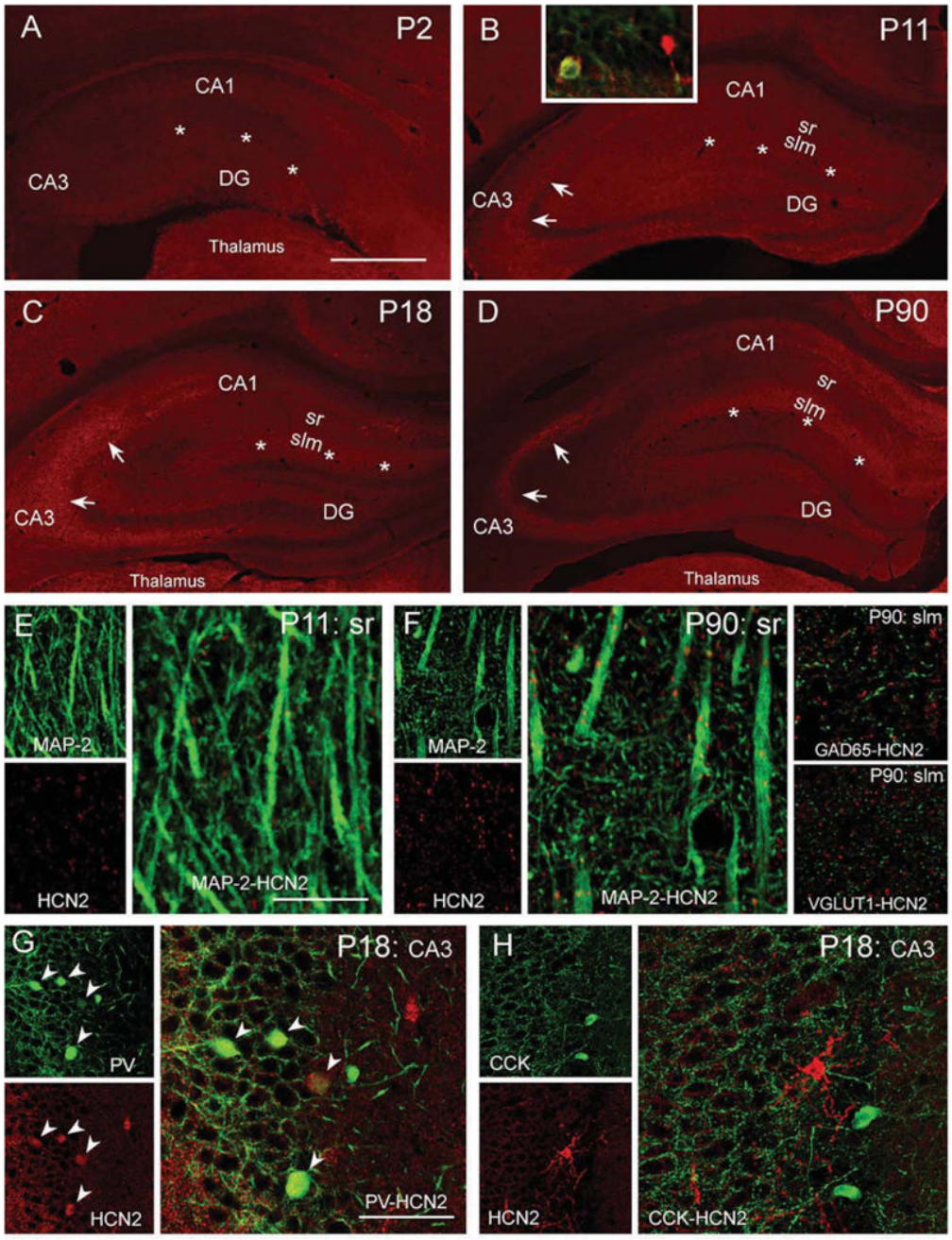

Figure 6.

Subcellular localization of HCN2 channels in developing hippocampus. (*A–D*) Low-magnification photographs demonstrate distribution of HCN2 channels on P2 (*A*), P11 (*B*), P18 (*C*), and P90 (*D*). In contrast to HCN1, HCN2 somata can easily be discerned in the P11 CA1 pyramidal cell layer, in both PV+ interneurons and PV–, presumed pyramidal, neurons. Localization of HCN2 channels in dendritic field of CA1 is apparent later in hippocampal maturation, as confirmed by high-resolution dual labeling: (*E, F*) Dual labeling of HCN2 (red) and MAP-2 (green) reveals overlapping expression in CA1 stratum lacunosum-moleculare (slm) on P90 (*F*), but not on P11 (*E*), suggesting that, compared with HCN1 (Fig. 3), dendritic trafficking of HCN2 channels commences at a later stage of CA1

pyramidal cell differentiation. Note that the pattern of HCN2 immunoreactivity is more punctate than that of HCN1, but this does not delineate presynaptic location: HCN2 fails to colocalize to GABAergic (GAD65) or glutamatergic (VGLUT1) afferents to the dendrites in slm. (*G, H*) Similar to HCN1, HCN2 signal over the pyramidal cell layer in CA3 (arrows in *B,C*, and *D*) is attributable to expression of HCN2 channels in axons and terminals as well as somata of basket cells. PV+ (*G*, arrowheads) but never CCK+ basket cells (*H*) colocalize HCN2. sr, stratum radiatum; asterisks demarcate the hippocampal fissure. Confocal microscope virtual slice thicknesses: (*A*–D) = 15 μm, (*E, F*) (MAP-2-HCN2) = 1 μm. (*F*) (GAD65 and VGLUT) = 0.5 μm. Scale bar: (*A–D*) = 900 μm; (*E*) = 27 μm (left panels), 13.5 μm (right panel); (*F*) = 27 μm (left and right panels), 13.5 μm (middle panel); (*G, H*) = 120 μm (left panels), 60 μm (right panel).

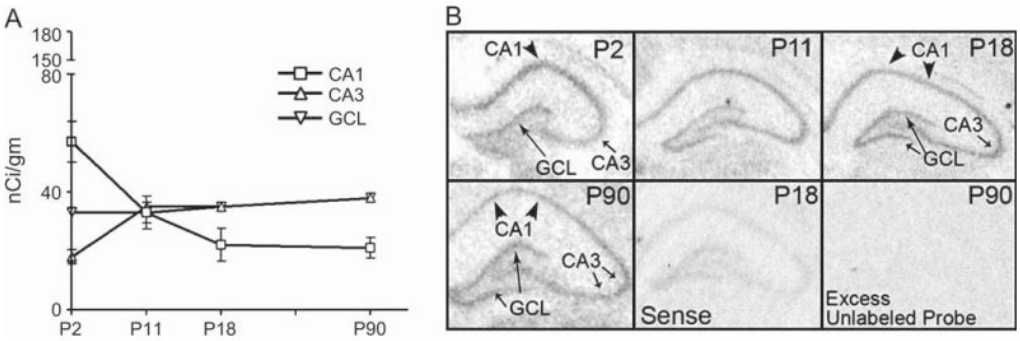

Figure 7.

Quantitative ISH analyses of HCN4 mRNA expression in developing hippocampus. (*A*) HCN4 mRNA is robustly expressed in neonatal CA1 pyramidal cell layer, where it decreases progressively with age (P2–P90: ~65%). In contrast, HCN4 mRNA expression is low in CA3 pyramidal cell layer and DG granule cell layer (GCL) on P2. With maturation expression increases 2-fold in CA3, whereas it remains constant in GCL. Note that HCN4 mRNA levels are lower than those of HCN1 (Fig. 1) and HCN2 (Fig. 4) and are shown on an expanded scale. (*B*) Representative autoradiographs show hippocampal HCN4 mRNA signal on P2, P11, P18, and P90 and the results of control ISH experiments using sense probe or excess (100×) unlabeled antisense probe in addition to labeled probe.

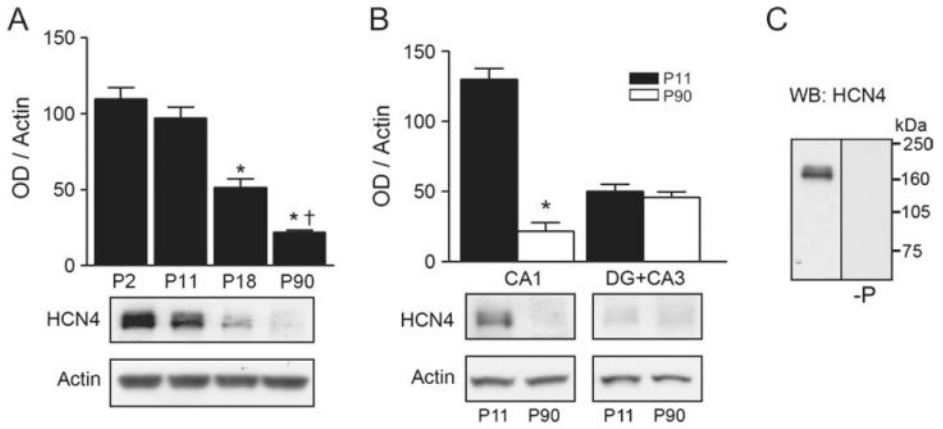

Figure 8.

Quantitative western blot analyses of HCN4 protein expression in developing hippocampus. (*A*) Top: Analysis of HCN4 protein levels in whole hippocampus reveals a progressive decrease of HCN4 protein expression between P2 and P90 (*denotes significance when compared with P2 and P11, †denotes significance when compared with P18; $P < 0.05$). Bottom: Representative western blot. Optical density (OD) of HCN4-immunoreactive bands was normalized to that of actin for each lane. (*B*) Top: Progression of HCN4 protein expression in isolated CA1 or DG + CA3 reflects the developmental profiles of the corresponding mRNA levels in these regions (compare with Fig. 7A). In CA1, HCN4 protein decreases ~80% (corresponding mRNA decrease: 57%), whereas protein levels remain unchanged in DG + CA3 (*denotes significance between groups; *t*-test: $P < 0.05$). Bottom: Representative western blots illustrate significantly higher HCN4 protein levels in CA1 at P11. (*C*) Immunoreactive-HCN4 bands have an apparent molecular weight of ~160 kDa (Notomi and Shigemoto 2004). Control experiments excluding the HCN4 antisera (-P) eliminate the immunoreactive bands.

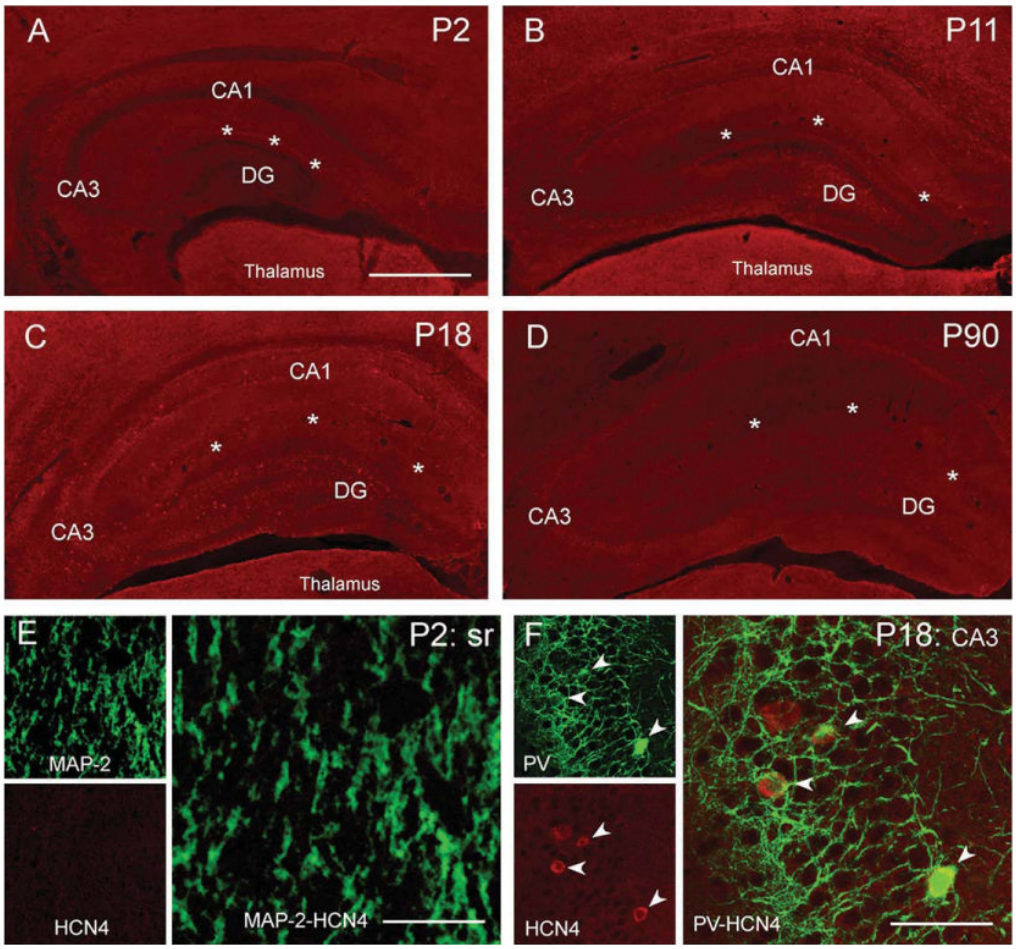

Figure 9.

Subcellular localization of HCN4 channels in developing hippocampus. (*A–D*) Low-magnification photographs show relatively low levels of HCN4 immunoreactivity in hippocampus on P2 (*A*), P11 (*B*), P18 (*C*), whereas HCN4 signal was poorly detectable on P90 (*D*). On P2, HCN4 signal was distributed over the pyramidal cell layer and weakly apparent in the dendritic fields of CA1 (*A*); however, dual labeling with MAP-2 did not provide evidence for a dendritic localization of these channels (*E*). HCN4 expression in interneurons was clearly visible on P18 (*C*). HCN4-immunoreactive interneurons were mainly associated with the pyramidal cell layer (*F*, arrowheads) and, similar to HCN1 and HCN2, coexpressed PV (*F*) but not CCK. In contrast to the situation with HCN1 and HCN2, HCN4 protein expression was found primarily in somata of PV-positive basket cells (*F*, arrowheads) and rarely in axonal terminals. slm, stratum lacunosum-moleculare; sr, stratum radiatum; asterisks demarcate hippocampal fissure. Virtual slice thickness: (*A–D*) = 15 μm; (*E*, *F*) = 1 μm. Scale bar: (*A–D*) = 900 μm; (*E*) = 27 μm (left panels), 13.5 μm (right panel); (*F*) = 120 μm (left panels), 60 μm (right panel).